

## THE IMPACT OF NATURAL CLIMATE VARIABILITY ON AIR CHEMISTRY AND REGIONAL AIR QUALITY

Volker Grewe

Institut für Physik der Atmosphäre, DLR-Oberpfaffenhofen, Germany,  
email: Volker.Grewe@dlr.de, tel.+49 (0)8153/28-2536

### Abstract

The modelling of the atmospheric composition on global scales has been significantly advanced during the last decade. A variety of processes are inherent in climate-chemistry models (CCMs), either resolved, parameterized or forced by boundary conditions. This ensures a better representation of the observed atmospheric composition and its variations, such as large scale climate phenomena (North-Atlantic Oscillation, El Nino/La Nina, etc), volcanic eruptions, solar effects, etc. Additionally, feedbacks between processes are included, like the impact of ozone, methane, and other species on radiation and dynamics, dynamics on emissions (e.g. lightning), and many others.

Dameris et al. (2005) present a troposphere-stratosphere simulation of the time period 1960 to 2000 using the CCM E39/C. This simulation includes observed sea-surface temperatures to account for effects like El Nino, and realistic planetary wave forcings, three major volcanic eruptions, the 11-year solar cycle, the Quasi-Biannual Oscillation (QBO), and varying emission of NO<sub>x</sub> and CFCs. The results show a good representation of the stratospheric and tropospheric dynamics, such as temperature trends, but also of the ozone layer, the development of the ozone hole, and tropospheric ozone in terms of composition and trend.

The application of a number of diagnostics (e.g. marked ozone tracers) allows the separation of the impact of various processes/emissions on tropospheric ozone. The simulated Northern Hemisphere tropospheric ozone budget is not only dominated by nitrogen oxide emissions and other ozone pre-cursors, but also by changes of the stratospheric ozone budget and the its flux into the troposphere, which tends to reduce the positive trend in ozone due to emissions from industry and traffic during the late 80s and early 90s.

Although the horizontal resolution is rather coarse in comparison to regional models, such kind of simulations provide useful and necessary information on the impact of large-scale processes and inter-annual / decadal variations on regional air quality.

*Keywords:* climate change, global modelling, air quality, ozone trends

### 1. Introduction

The chemical composition of the atmosphere shows a large variability on a variety of time scales. Additionally, systematic changes have been measured, which largely can be attributed to anthropogenic activities. Measurements at Hohenpeissenberg (Southern

Germany) show stratospheric (at 20 km) ozone depletion by 16% compared to 1967 and tropospheric (at 5 km) ozone increase by 30% for the same time period (DWD, 2005; <http://www.dwd.de/de/FundE/Observator/MOHP/hp2/ozon/trend3.htm>). The tropospheric time series shows a slight decrease from the mid 80s onwards, which is not fully understood. Besides these long-term changes, there are clear year to year variations. The natural variability has to be understood in order to be able understand the measured trends. The separation of trends from variability enables the attribution of ozone changes to human activity.

Figure 1 shows the principle interactions between chemistry and dynamics and gives examples for climate-chemistry interactions. The stratospheric general circulation is characterized by an uprising in the tropics and downward transport at high latitudes. One of the main stratospheric ozone production regions is clearly the tropical mid stratosphere, where ozone production and destruction leads to a photochemical equilibrium of ozone. In the troposphere, ozone concentration is dominated by ozone influx from the stratosphere and by ozone production via  $\text{NO}_2$  photolysis. These processes are changing with time, e.g. the 11-year sun spot cycle significantly effects the stratospheric ozone production and concentration (WMO, 2003). In the tropical troposphere the  $\text{NO}_x$  and ozone concentration largely depends on the lightning produced  $\text{NO}_x$  (Grewé, 2004). The El Nino/La Nina phenomenon, is the most important natural climate variability in the tropics affecting the lightning occurrence and therefore also the ozone concentration (climate-chemistry interaction). Looking for air quality, it is clear that the near surface concentrations are only covering a small fraction of the air masses in the described atmospheric system. However, those concentrations are not only locally determined, but there are interactions on a global scale.

In this paper, a climate-chemistry simulation for the troposphere and stratosphere is analysed, which covers the period 1960 to 2000 (Dameris et al., 2005). Special diagnoses are applied in order to separate individual effects. Section 2 introduces briefly the model system and the experimental set-up. Section 3 describes the methodologies applied to attribute ozone changes to various atmospheric processes. Section 4 concentrates on stratospheric variability and its impact on the tropospheric ozone influx, whereas the tropospheric variability is analysed in Section 5.

## 2. Model description and experimental set up

The applied global climate-chemistry model E39/C (Hein et al., 2001) consists of the troposphere-stratosphere climate model ECHAM4.L39(DLR) (Land et al., 1999) and the troposphere-stratosphere chemistry module CHEM (Steil et al., 1998). The climate model is a derivate of the standard ECHAM4 model (Roeckner et al., 1996), with a higher vertical resolution especially at tropopause levels (~700 m) to better represent processes and gradients in this region. CHEM includes homogeneous and heterogeneous stratospheric reactions, as well as the basic tropospheric chemistry. A speciality of the model is the amount of allowed interactions, e.g. the hydrological cycle is directly coupled to the chemistry scheme, photolysis scheme, wash-out and lightning; Changes in the composition of radiative active species directly affect dynamics via the radiation scheme. The model system has been intensively validated against measurements including a variety of international validation activities (Brunner et al., 2003, Brunner et

al., 2005, Austin et al. 2003, Shine et al. 2003) and has been applied for a variety of scientific questions concerning the future development of the ozone layer (Schnadt et al., 2002), aircraft impacts (Grewe et al., 2002; and references therein), etc.

In this paper a simulation from 1960 to 2000 is analysed, which is fully described in Dameris et al. (2005). It includes a variety of changing boundary conditions, like monthly mean observed sea surface temperatures, the 11-year solar cycle, the Quasi-Biennial-Oscillation, three major volcanic eruptions, which affect the stratospheric aerosol loading, and the emissions of CO<sub>2</sub>, CH<sub>4</sub>, N<sub>2</sub>O, CFCs, NO<sub>x</sub> (biomass burning, traffic, ships, soils, lightning, industry, air traffic).

### 3. Methodologies

In order to separate processes affecting the ozone concentration two different methodologies are applied: (1) A NO<sub>x</sub>-ozone tracking diagnosis (Grewe, 2004) and (2) ozone origin diagnosis (Grewe, 2005). For the NO<sub>x</sub>-ozone tracking diagnosis 8 sources for NO<sub>x</sub> are specified (lightning, biomass burning, soils, industry, land transportation, ships, air traffic and stratospheric N<sub>2</sub>O degradation, see Figure 2). To each of these sources a NO<sub>y</sub> tracer is assigned in addition to the chemical species in the module CHEM, which experiences its specific emission and NO<sub>y</sub> loss terms proportional to the total NO<sub>y</sub> loss. To each NO<sub>y</sub> tracer an ozone tracer is assigned, which experiences an ozone production proportional to the ratio of specific NO<sub>y</sub> to total NO<sub>y</sub> concentration multiplied by the total ozone production via NO<sub>2</sub> photolysis. A further ozone tracer is included to account for ozone production by O<sub>2</sub> photolysis (mainly stratosphere). A detailed description and error analysis can be found in Grewe (2004).

The second diagnosis is applied to identify regions of ozone production. The idea is similar to the previous. Nine regions are defined (see Figure 3) to which an ozone tracer is linked. Each tracer experiences ozone production in this region only, and losses proportional to its concentration. Figure 3 shows how the individual ozone origin tracers are transported through the atmosphere and how they are chemically destroyed. For both diagnoses, the sum of all ozone tracers equals the simulated ozone field. Therefore, the diagnoses allow the interpretation, how much of this ozone field is produced by a specific NO<sub>x</sub> emissions (1<sup>st</sup> diagnosis) and where the ozone is actually produced (2<sup>nd</sup> diagnosis).

### 4. The role of the stratosphere and stratospheric influx

The lifetime of ozone in the stratosphere varies from region to region. In the mid tropical stratosphere, its lifetime is so short that ozone is chemically controlled. At high latitudes or at tropopause levels, dynamics control the distribution. Therefore, the ozone column (Figure 4) is characterized by either pattern of variability, chemically and dynamically induced. An overview of those effects present in the simulation 1960 to 2000 can be found in Dameris et al. (2005). Figure 4 and 5 summarize the main effects. On the Northern Hemisphere a high inter-annual variability can be found, which is in reasonable agreement with observational data and caused by propagating planetary waves, which are less present on the Southern Hemisphere. The ozone hole is clearly visible from the beginning of the 80s and with values below 150 DU in the 90s. Variability patterns can

better be identified by deseasonalizing the time series (Figure 5). The 11-year solar cycle can be identified in the tropics with higher values at solar maximum, e.g. around 1980, and the effect of the QBO with higher values during west phase, because the induced secondary circulation reduces the tropical ascent.

The variations in stratospheric ozone also affect the ozone influx into the troposphere. Figure 6 shows the ozone flux calculated according to Wei (1987) (also described in Grewe and Dameris, 1996). The total amount of ozone exchanged into the troposphere of around 440 Tg per year is in good agreement with observational data (e.g. Murphy and Fahey, 1994: 475 Tg/a; Olsen et al. 2004: 500 Tg/a). By decomposing the total flux into Northern and Southern Hemisphere contributions (red and blue curves) it becomes clear that the 11 year solar cycle can better be identified on the Southern Hemisphere, whereas on the Northern Hemisphere the year to year variability is larger. The interannual variability, in terms of min-max values, amounts to  $\pm 10$  Tg/month, which is around  $\pm 30\%$ .

In order to explain these variations in more detail the ozone origin diagnosis can be applied. Figure 8 shows for the Northern (top) and Southern Hemisphere (bottom) and for each season from where the ozone originates, which is transported into the troposphere. On the Northern Hemisphere the ozone influx mainly originates from the regions NHMS (Northern Hemisphere mid-stratosphere), TRMS (tropical mid-stratosphere), and TRTS (tropical troposphere). Since the NHMS is dominated by a huge year-to-year variability, also the Northern Hemisphere ozone influx experiences this variability. The Southern Hemisphere ozone influx originates mainly from the regions TRTS (tropical troposphere), SHMS (Southern Hemisphere mid-stratosphere), and TRLS (tropical troposphere). The year-to-year variability of ozone in the SHMS region is much lower than in the NHMS region, because of the smaller planetary wave activity. Instead, the variability induced by the solar cycle is dominating the variability of ozone in the SHMS and consequently also in the Southern Hemisphere ozone influx.

## 5. Tropospheric variability

The variability of the ozone concentration in the troposphere is influenced by both stratospheric and tropospheric processes (Fig. 1). The discussion will focus on two regions: the tropical upper troposphere and the Northern Hemisphere lower troposphere, marked as black boxes in Figure 2. Figure 8 shows the temporal development of ozone in the upper tropical troposphere, including the ozone partitioning, resulting from the various  $\text{NO}_x$  emissions derived by the  $\text{NO}_x$ -ozone diagnostic (Sec. 3). Clearly lightning  $\text{NO}_x$  emissions dominate the ozone concentration in that region. Stratospheric ozone (red curved, not to be confused with air traffic) is the second most important contributor, followed (only in the 90s) by industrial emissions. The interannual variability is dominated by the variability in lightning occurrence and stratospheric dynamics. This may be misleading, since the anthropogenic  $\text{NO}_x$  emissions included in the model do not have an interannual variability, a stepwise linear change in the global emission rate is assumed, though. The lower panel of Figure 8 shows the deseasonalised ozone changes produced by lightning  $\text{NO}_x$  emissions and stratospheric influx (curves are shifted by 5 Tg/month to separate the lines). Additionally the ozone influx (see also Figure 6) and the El Nino index is shown. Clearly, in the upper troposphere, ozone originated from the

stratosphere follows the ozone influx, sometimes with some temporal shift, which is due to variations in the photochemical activity, e.g. produced by the seasonal cycle. This implies that the variability of ozone in the upper tropical troposphere can directly be attributed to the variability of the Northern Hemisphere mid stratosphere dynamics, e.g. maximum values exceeding 15 Tg/month during the 60s and 70s (Figure 8 top panel) are correlated to positive anomalies of total ozone (Figure 5). This is also true for the solar cycle, with higher values around 1970, 1980 and 2000.

El Nino, as an example for tropospheric climate variability, affects tropical lightning, both in terms of location of occurrence and total amount of NO<sub>x</sub> emitted. The applied diagnostic provides the possibility to attribute the ozone variations directly to this climate variability pattern.

The interannual variability of ozone caused by stratospheric dynamics is in the order of  $\pm 4\%$ , whereas the variability produced by the El Nino phenomenon is in the order of  $\pm 2-3\%$ .

In the Northern Hemisphere lower troposphere (Figure 9, top panel), the ozone concentration is dominated by industry (~15 Tg), surface traffic (~12 Tg), lightning (~10 Tg) and stratospheric intrusion (~7 Tg). The interannual variability (Figure 9, lower panel) is dominated by the stratospheric intrusions. Again, this is partly due to the underestimated interannual variability in the emission data. The ozone increase of around 30% from the early 60s shows a stepwise behaviour, with almost constant values during the 80s. This has two reasons: First, the anthropogenic NO<sub>x</sub> emissions included in the model are assumed to have smaller increase rates during that period, which is visible looking at the ozone changes caused by industrial NO<sub>x</sub> emissions. Second, the ozone contribution from the stratosphere is decreasing by approximately 5% during that time, partly caused by the stratospheric ozone depletion.

## 6. Summary

The atmospheric concentration of ozone shows a large variability in many parts of the atmosphere. To better understand the driving parameters for this variability and to be able to attribute variability and changes to natural climate variability and anthropogenic changes a multi-decadal simulation (1960 to 2000) has been performed, employing realistic natural forcings, like El Nino, QBO, volcanoes, solar cycle. Additionally, diagnostic tools have been applied to attribute ozone changes and variations to specific NO<sub>x</sub>/ozone sources and to relate ozone concentrations to the regions, where this ozone is actually produced.

It has been shown that the stratospheric dynamics and the main stratospheric ozone variability pattern are well reproduced (Dameris et al., 2005). A total trend of approximately 20 DU is simulated, which mainly results from CFC emissions, but is also caused by 10% by an increase in water vapour due to tropospheric warming leading to a moistening of the stratosphere (Stenke and Grewe, 2005).

The influx of ozone from the stratosphere into the troposphere depends on the stratospheric circulation and the chemical stratospheric ozone production. Applying the ozone origin diagnostics leads to the result that the variability of the ozone influx into the troposphere on the Northern Hemisphere is dominated by stratospheric dynamics and on the Southern Hemisphere by variations of the ozone production caused by the solar cycle.

This directly produces a variability in tropospheric ozone of  $\pm 4\%$ , which is most pronounced in the tropics. Another climate variability pattern is forced by the El Nino phenomenon, which increase lightning occurrence and lightning  $\text{NO}_x$  emissions and leads to an inter-annual ozone variability of around  $\pm 3\%$ .

On the Northern Hemisphere, lower troposphere, the region which is related to air quality aspects, ozone is mainly produced by industry  $\text{NO}_x$  emissions. Since the anthropogenic emissions show an increase during the simulation period, also the ozone produced by those emissions shows a similar behaviour, i.e. a total increase of 30% (relative to the total ozone) and a smaller increase during the 80s. Since the contribution from stratospheric ozone is decreasing by 5% (with respect to total ozone) during the 80s, the overall increase amounts only to 25%, with a constant value during the 80s. Since reliable global emission data were not available for the simulation, the results are clearly limited by the rather coarse assumptions concerning the anthropogenic emissions. However, the results clearly indicate that the near surface ozone burden, which is an air quality aspect, is to some extent affected by stratospheric processes and that ozone trends can be weakened and strengthened by stratospheric processes and climate-chemistry interactions (e.g. El Nino).

On the other hand, the simulation does not include small scale processes, normally resolved by air quality/regional models. A number of feedbacks are possible, such as plume conversion processes in the vicinity of cities, etc. It will be a challenge to include these effects in future climate-chemistry simulations.

## 7. References

- Austin, J. , Shindell, D., Beagley, S. R., Brühl, C., Dameris, M., Manzini, E., Nagashima, T., Newman, P., Pawson, S., Pitari, G., Rozanov, E., Schnadt, C. and Shepherd, T. G. Uncertainties and assessments of chemistry-climate models of the stratosphere, *Atmos. Chem. Phys.*, 3, 1-27, 2003.
- Brunner, D., J. Staehelin, H. L. Rogers, M. O. Köhler, J. A. Pyle, D. Hauglustaine, L. Jourdain, T. K. Berntsen, M. Gauss, I. S. A. Isaksen, E. Meijer, P. van Velthoven, G. Pitari, E. Mancini, V. Grewe, and R. Sausen: An evaluation of the performance of chemistry transport models by comparison with research aircraft observations. Part 1: Concepts and overall model performance. *Atmos. Chem. Phys.*, 3, 1609-1631, 2003.
- Brunner, D., Staehelin, J. , Rogers, H. , Köhler, M. , Pyle, J. , Hauglustaine, D. , Jourdain, L. , Berntsen, T., Gauss, M. , Isaksen, I. , Meijer, E. , Velthoven, P. , Pitari, G. , Mancini, E. , Grewe, V. and Sausen, R. Atmospheric Chemistry and Physics, An evaluation of the performance of chemistry transport models - Part 2: Detailed comparison with two selected campaigns, *Atmos. Chem. Phys.* 5, 107-129, 2005.
- Dameris, M., Grewe, V., Ponater, M., Deckert, R., Eyring, V., Mager, F., Matthes, S., Schnadt, C., Stenke, A., Steil, B., Brühl, C., and Giorgetta, M. Long-term changes and variability in a transient simulation with a chemistry-climate model employing realistic forcings, *ACPD* 5, 2297-2353, 2005.
- Grewe, V., Technical Note: A diagnostic for ozone contributions of various  $\text{NO}_x$  emissions in multi-decadal chemistry-climate model simulations, *Atmos. Chem. Phys.* 4, 327-342, 2004.
- Grewe, V., The origin of ozone: Identifying regions of dominant ozone production, in preparation, 2005.

- Grewe, V., M. Dameris, C. Fichter, R. Sausen, Impact of aircraft NO<sub>x</sub> emissions. Part 1: Interactively coupled climate-chemistry simulations and sensitivities to climate-chemistry feedback, lightning and model resolution, *Meteorol. Z.*, 3, 177-186, 2002.
- Grewe, V. and M. Dameris, Calculating the global mass exchange between stratosphere and troposphere, *Ann. Geophysicae*, 14, 431-442, 1996.
- Hein, R., M. Dameris, C. Schnadt, C. Land, V. Grewe, I. Köhler, M. Ponater, R. Sausen, B. Steil, J. Landgraf, C. Brühl, Results of an interactively coupled atmospheric chemistry-general circulation model: Comparison with observations, *Ann. Geophys.* 19, 435-457, 2001.
- Land, C., M. Ponater, R. Sausen, E. Roeckner, The ECHAM4.L39(DLR) atmosphere GCM, Technical description and climatology, DLR-Forschungsbericht 1991-31, 45 pp., ISSN 1434-8454, Deutsches Zentrum für Luft- und Raumfahrt, Köln, Germany, 1999.
- Murphy, D.M., and Fahey, D.W., An estimate of the flux of stratospheric reactive nitrogen and ozone into the troposphere. *J. Atmos. Sci.*, 51, 654-673, 1994.
- Olsen, M.A., Schoeberl, M.R., and Douglass, A.R., Stratosphere-troposphere exchange of mass and ozone, *JGR* 109, doi:10.1029/2004JD005186, 2004.
- Roeckner, E., K. Arpe, L. Bengtsson, M. Christoph, M. Claussen, L. Dümenil, M. Esch, M. Giorgetta, U. Schlese, U. Schulzweida, The atmospheric general circulation model ECHAM4: Model description and simulation of present-day climate, MPI-Report 218, ISSN 0937-1060, Max-Planck-Institut für Meteorologie, Hamburg, Germany, 1996.
- Schnadt C., M. Dameris, M. Ponater, R. Hein, V. Grewe, and B. Steil, Interaction of atmospheric chemistry and climate and its impact on stratospheric ozone, *Climate Dynamics*, 18, 501-517, 2002.
- Shine, K.P., M.S. Bourqui, P.M. de F. Forster, S.H.E. Hare, U. Langematz, P. Braesicke, V. Grewe, M. Ponater, C. Schnadt, C.A. Smith, J.D. Haigh, J. Austin, N. Butchart, D. Shindell, W.J. Randell, T. Nagashima, R.W. Portmann, S. Solomon, D. Seidel, J. Lanzante, S. Klein, V. Ramaswamy, M.D. Schwarzkopf. A comparison of model-predicted trends in stratospheric temperatures, *Quarterly Journal of the Royal Meteorological Society*, 129, 1565-1588, 2003.
- Steil, B., M. Dameris, C. Brühl, P.J. Crutzen, V. Grewe, M. Ponater, and R. Sausen, Development of a chemistry module for GCMs: first results of a multiannual integration, *Ann. Geophys.* 16, 205-228, 1998.
- Stenke, A. and Grewe, V. Simulation of stratospheric water vapor trends: impact on stratospheric ozone chemistry, *ACPD* 4, 6559-6602, 2004.
- Wei, M.-Y., A new formulation of the exchange of mass and trace constituents between the stratosphere and troposphere, *J. Atmos. Sci.* 44, 3079-3086, 1987.
- WMO (World Meteorological Organization): Scientific Assessment of Ozone depletion: 1998, Global Ozone Research and Monitoring Project, Rep. 44, 1999.
- WMO (World Meteorological Organization): Scientific Assessment of Ozone depletion: 2002, Global Ozone Research and Monitoring Project, Rep. 47, 2003.

## 8. Figures

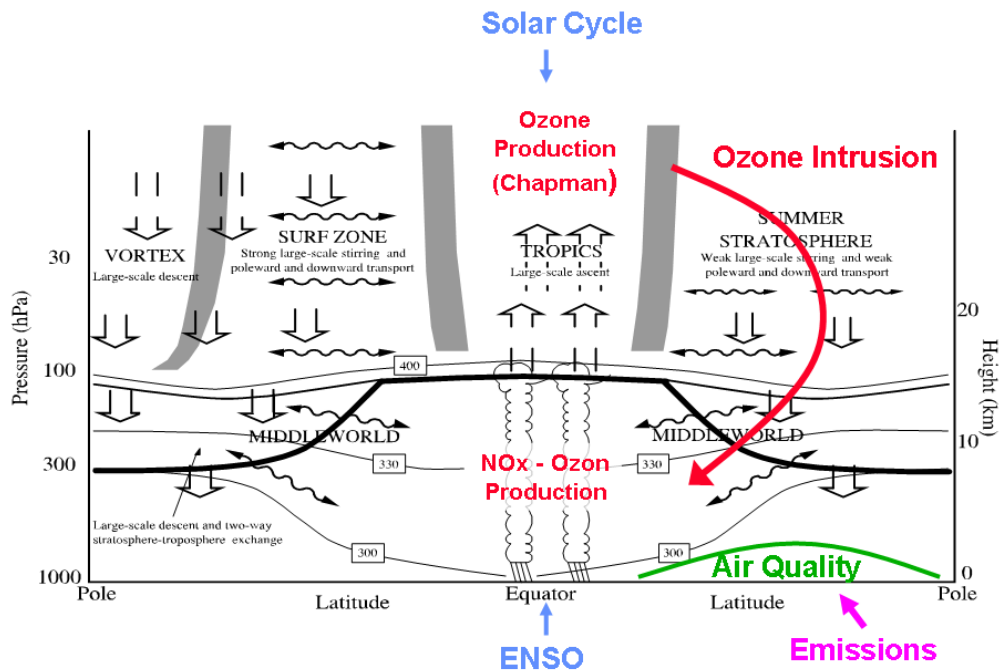


Fig. 1: Sketch of the main atmospheric processes. Heavy thick lines mark the tropopause; shaded areas barriers to transport, arrows large-scale vertical exchange; and thin lines mark isentropes [K]. The coloured text describes the main focus of this paper. Figure adapted from the WMO (1999).

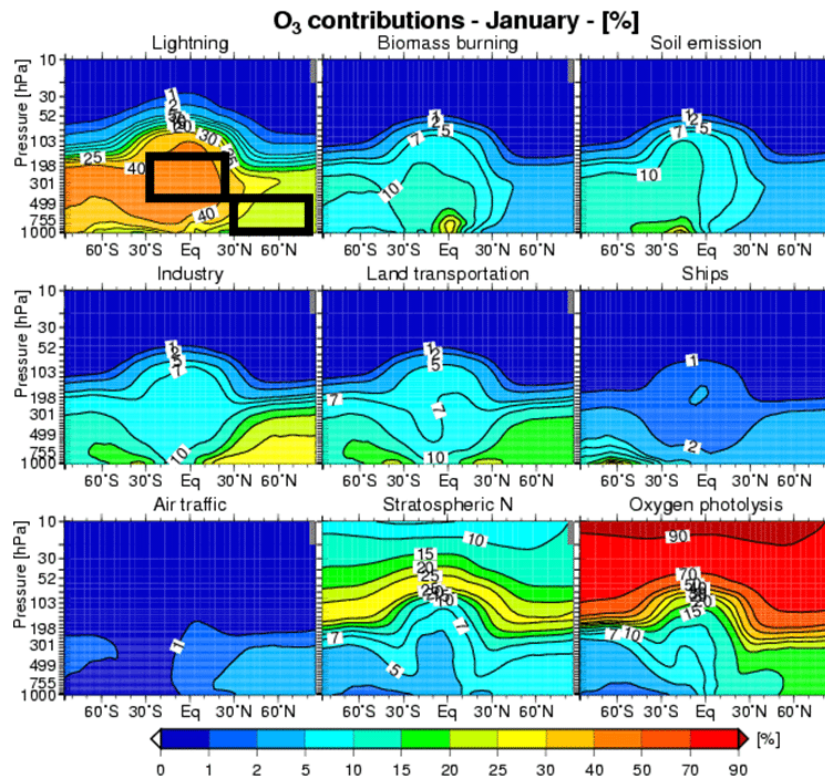


Fig. 2: Decomposition [%] of the zonal mean simulated ozone into the basic sources of ozone, i.e. due to  $\text{NO}_2$  photolysis caused by  $\text{NO}_x$  emissions from lightning, biomass burning, soils, industry, surface traffic, ships, air traffic, stratospheric production of nitrogen and the photolysis of  $\text{O}_2$ . Boxes mark areas further discussed in the text (see also Fig. 8 and Fig. 9). Figure adapted from Grewe (2004).

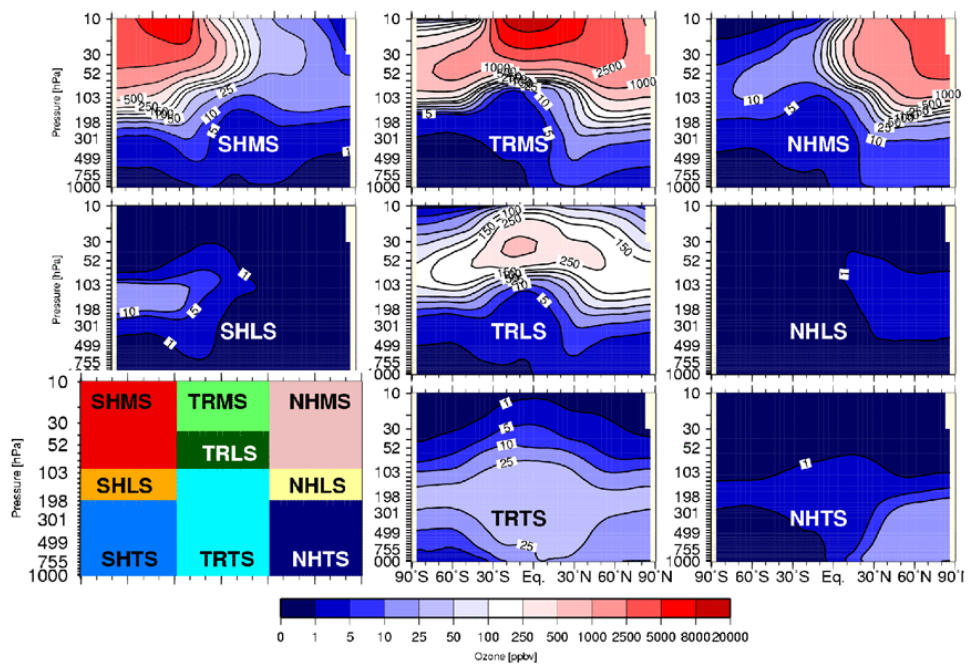


Fig. 3: Decomposition [ppbv] of the zonal mean simulated ozone into nine ozone fields representing ozone produced in nine different regions. The nine regions are displayed lower left and abbreviated with four letters: the first two describe Southern Hemisphere (SH), Tropics (TR), and Northern Hemisphere (NH) and the second two letters Mid-Stratosphere (MS), Lower Stratosphere (LS), and Troposphere (TS), respectively. Figure is adapted from Grewe (2005).

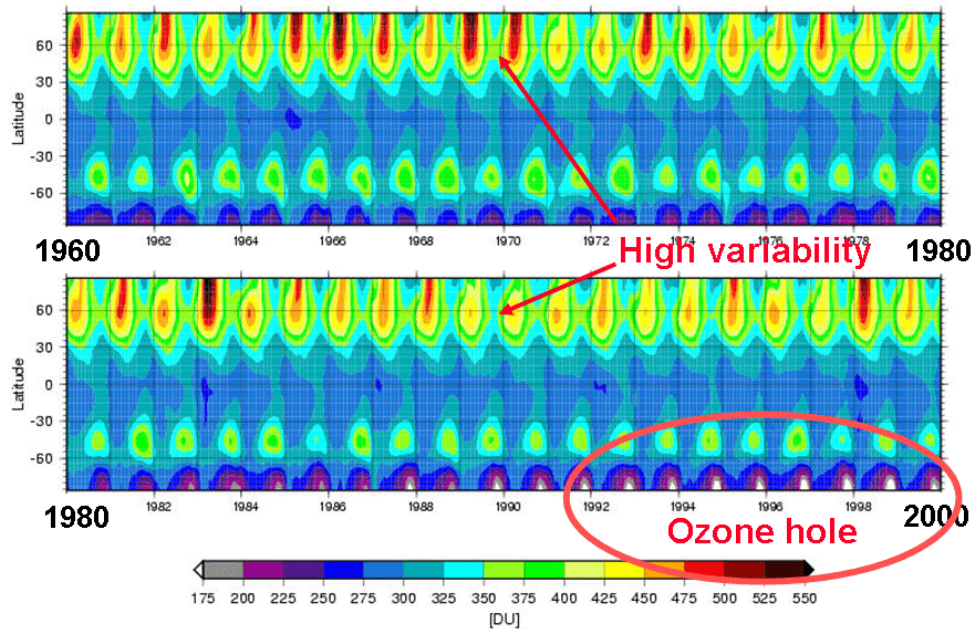


Fig. 4: Zonal mean simulated total ozone field [DU] from 1960 to 2000. Figure adapted from Dameris et al. (2005).

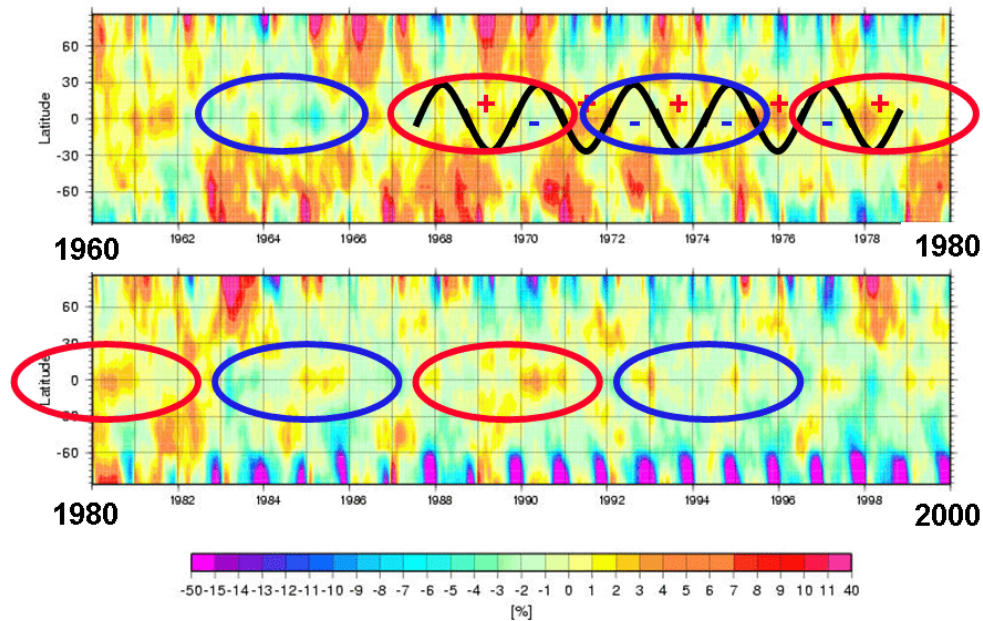


Fig. 5: De-seasonalized zonal mean simulated total ozone field [%] from 1960 to 2000, as an anomaly to the period 1964 to 1980. Figure adapted from Dameris et al. (2005). The black line and plus (west phase) and minus (east phase) signs indicate the QBO, the ellipses mark the 11-year sun spot cycle (blue: solar min; red: solar max).

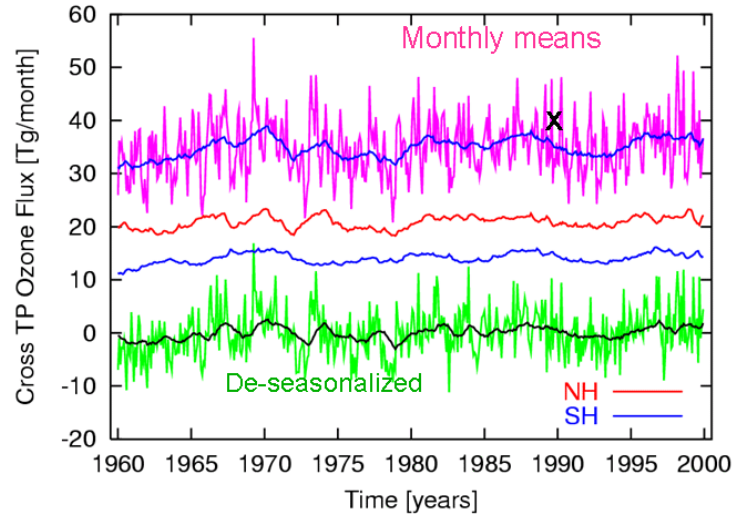


Fig. 6: Simulated monthly mean cross tropopause ozone flux [Tg/month] (magenta) and a 25 month running mean (blue). Red and blue curves mark the Northern and Southern Hemisphere contributions, respectively. The green line shows the de-seasonalized flux with a running mean overlaid (black line). The cross marks an estimate based on observational data (Murphy and Fahey, 1994).

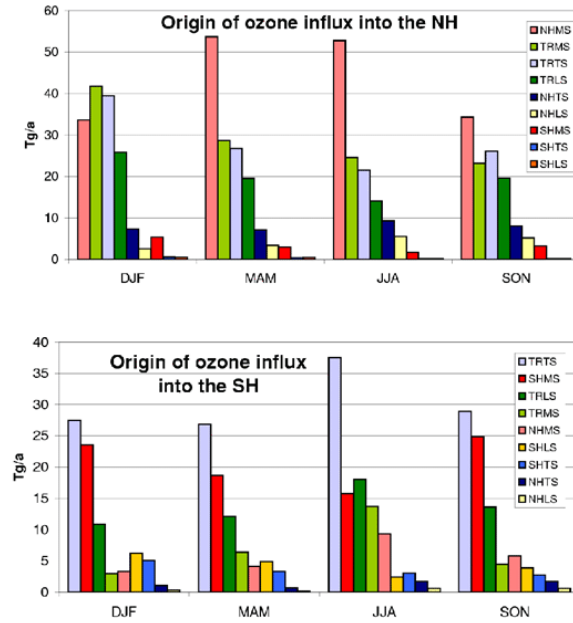


Fig. 7: Decomposition of the ozone influx into ozone contributions from various regions (see Fig. 3) for the 4 seasons and for Northern (top) and Southern (bottom) hemisphere. Figure adapted from Grewe (2005).

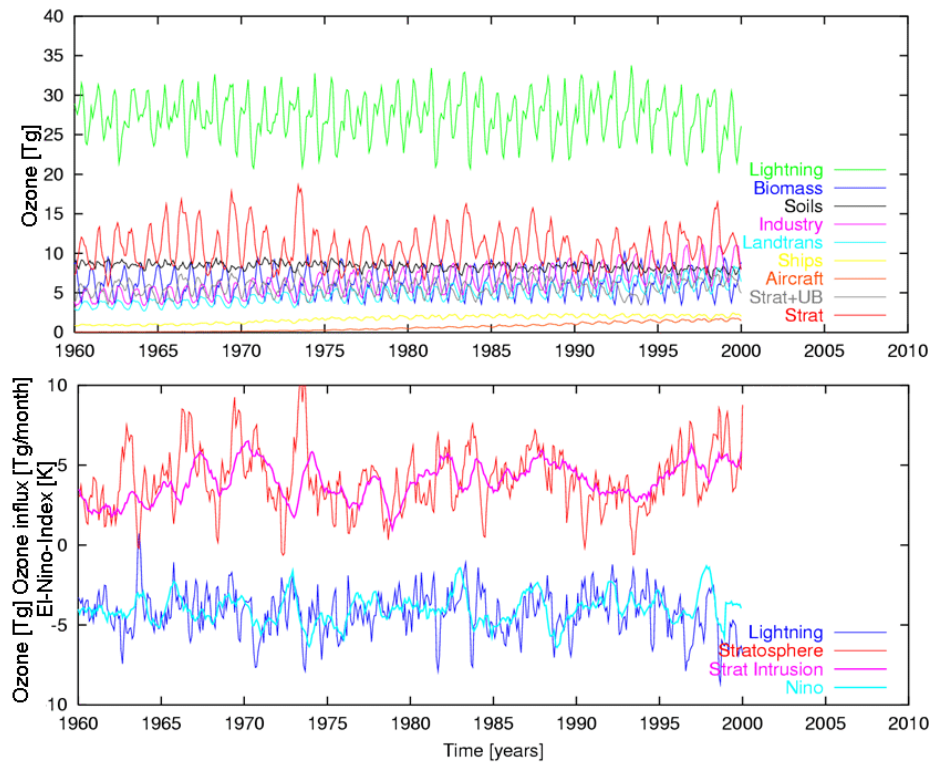


Fig. 8: Upper troposphere tropical ozone budgets [Tg]. Top: Decomposition into various ozone sources (see Fig. 2). Bottom: De-seasonalized anomalies [Tg] for stratospheric ozone (red) and lightning (dark blue) with a vertical off-set to separate the lines. Overlaid are the stratospheric ozone intrusion [Tg/month] (magenta; see also Fig. 6) and the El-Nino3 Index [K] (light blue).

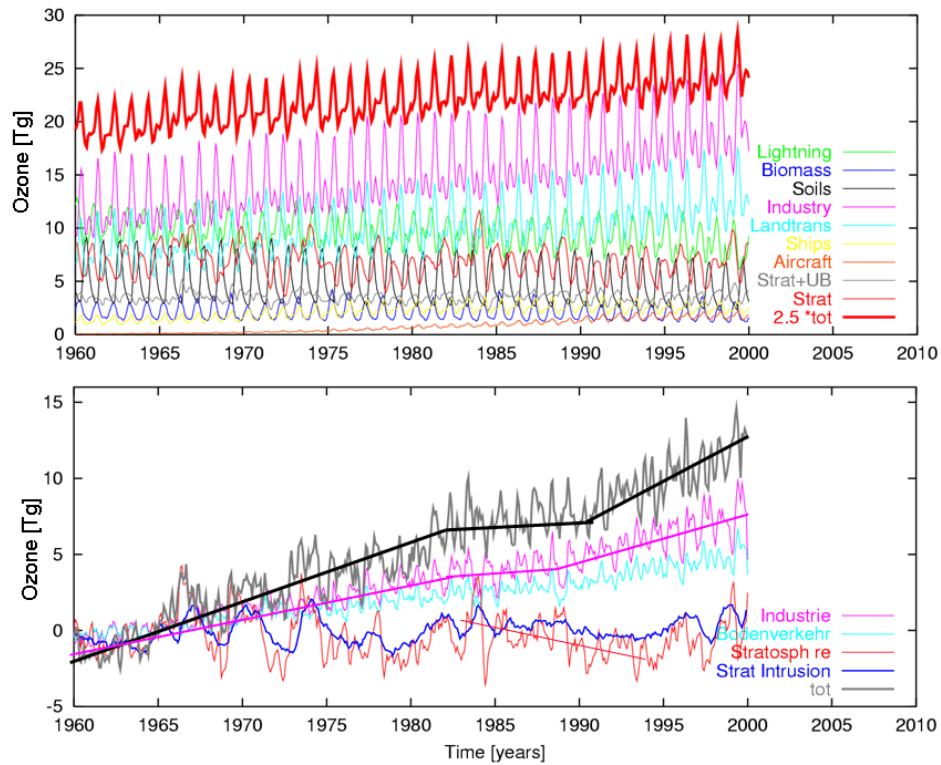


Fig. 9: Lower troposphere Northern Hemisphere ozone budgets [Tg]. Top: Decomposition into various ozone sources (see Fig. 2). Bottom: De-seasonalized anomalies [Tg] for stratospheric ozone (red), industry (magenta), surface traffic (light blue) and total ozone (grey). Overlaid in blue are the Northern Hemisphere ozone intrusion anomalies [Tg/month].